Exotic neutron-rich medium-mass nuclei with realistic nuclear forces

Naofumi Tsunoda,[1] Takaharu Otsuka,[1,2,3,4] Noritaka Shimizu,[1]
Morten Hjorth-Jensen,[5,6] Kazuo Takayanagi,[7] and Toshio Suzuki[8]

[1] *Center for Nuclear study, the University of Tokyo, 7-3-1 Hongo, Bunkyo-ku, Tokyo, Japan*
[2] *Department of physics and Center for Nuclear Study, the University of Tokyo, 7-3-1 Hongo, Bunkyo-ku, Tokyo, Japan*
[3] *National Superconducting Cyclotron Laboratory, Michigan State University, East Lansing, MI, 48824, USA*
[4] *Instituut voor Kern- en Stralingsfysica, Katholieke Universiteit Leuven, B-3001 Leuven, Belgium*
[5] *National Superconducting Cyclotron Laboratory and Department of Physics and Astronomy, Michigan State University, East Lansing, MI, 48824, USA*
[6] *Department of Physics, University of Oslo, N-0316 Oslo, Norway*
[7] *Department of Physics, Sophia University, 7-1 Kioi-cho, Chiyoda-ku, Tokyo 102, Japan*
[8] *Department of Physics, College of Humanities and Sciences, Nihon University, Sakurajosui 3, Setagaya-ku, Tokyo 156-8550, Japan*

(Dated: September 20, 2016)

We present the first application of the newly developed EKK theory of the effective nucleon-nucleon interaction to shell-model studies of exotic nuclei, including those where conventional approaches with fitted interactions encounter difficulties. This EKK theory enables us to derive the interaction suitable for several major shells (sd+pf in this work). By using such effective interaction obtained from the Entem-Machleidt QCD-based χN^{3}LO interaction and the Fujita-Miyazawa three-body force, the energies, E2 properties and spectroscopic factors of low-lying states of neutron-rich Ne, Mg and Si isotopes are nicely described, as the first shell-model description of the "island of inversion" without fit of the interaction. The long-standing question as to how particle-hole excitations occur across the sd-pf magic gap is clarified with distinct differences from the conventional approaches. The shell evolution is shown to be endorsed by the present study.

PACS numbers: 21.30.Fe, 21.60.Cs, 27.30.+t
Keywords: Effective interaction, shell model, island of inversion, shell evolution, exotic nuclei

Introduction. – The nuclear shell model [1, 2] provides a unified and successful description of both stable and exotic nuclei, as a many-body framework which can be related directly to nuclear forces. Exotic nuclei are located far from the β-stability line on the Segrè chart, exhibiting very short life times, mainly due to an unbalanced ratio of proton (Z) and neutron (N) numbers. Exotic nuclei differ remarkably in some other aspects from their stable counterparts, providing us with new insights in understanding atomic nuclei and nuclear forces [3, 4, 5]. As experimental data on exotic nuclei are, in general, less abundant compared to stable nuclei, theoretical calculations, interpretations and predictions play an ever increasing role.

Shell-model (SM) calculations handle the nuclear forces in terms of two-body matrix elements (TBMEs). In the early days, TBMEs were empirically determined in order to reproduce certain observables. A well-known example is the effective interaction for p-shell nuclei by Cohen and Kurath [6]. A breakthrough towards more microscopically-derived TBMEs was achieved by Kuo and Brown for sd-shell nuclei [7]. Although basic features of the nucleon-nucleon (NN) force for the SM calculation are included in these effective interactions, empirical adjustments of TBMEs were needed in order to reproduce various observables [8, 9, 10].

These effective interactions were all derived for a Hilbert space represented by the degrees of freedom of one major (oscillator) shell. As we move towards exotic nuclei, some new features and phenomena arise. A notable example can be the shell evolution due to nuclear forces between a proton and a neutron in different shells [5, 11, 12]. This leads to significant particle-hole excitations between two shells, for example, in Z=8-14 neutron-rich exotic nuclei [3, 4, 5, 9, 11, 12, 13, 14, 15, 16, 17]. A microscopic understanding of many of these phenomena requires the degrees of freedom of at least two major shells.

To derive SM effective Hamiltonians is a challenge to nuclear theory. Several attempts have been made recently in this direction [18, 19, 20, 21, 22, 23, 24], while the issue of two major shells has been kept open.

The aim of this work is to derive SM interaction for the model space comprised of the sd and pf shells based on the so-called Extended Kuo-Krenciglowa (EKK) method [25, 26, 27], and to apply it to exotic neutron-rich Ne, Mg and Si isotopes. These are nuclei in and around the so-called "island of inversion" [14], where the degrees of freedom of sd and pf shells are essential. We thus present, in this Letter, the first application of the EKK method to actual cases. We include also three-nucleon force (3NF) since it has been shown to play an important role in reproducing basic nuclear properties [28, 29, 30, 31, 32].

Hamiltonan and model spaces. – The many-body perturbation theory (MBPT) has been the standard many-body method for deriving effective interactions, as discussed in Refs. [33, 34, 35, 36, 37]. The conventional MBPTs, for instance, Kuo-Krenciglowa (KK) method [33, 34, 35], are constructed for degenerate single-particle states in the model space, which usually refers to one major shell [33, 34, 35, 36, 37]. The present model space, however, includes all single-particle states of the *sd* and the *pf* shells, labeled *sdpf* hereafter. This leads to possible divergencies when constructing an effective interaction with conventional MBPTs due to non-degeneracies of the single-particle states. A practical, but not satisfactory way to circumvent such divergencies has been to enforce in an *ad hoc* way degenerate single-particle energies for all involved single-particle states spanning a model space, see for example Refs. [29, 38, 39]. Employing the EKK method as done in this work, removes the above-mentioned divergency problems and allows for a correct treatment of the different single-particle energies [27]. Starting from a Hamiltonian which contains kinetic energy and a two-body NN interaction and following the formalism described in Ref. [27], we can define an effective Hamiltonian through

$$H_{\rm eff} = H_{\rm BH}(\xi) + \sum_{k=1}^{\infty} \frac{1}{k!} \frac{{\rm d}^k \hat{Q}(\xi)}{{\rm d}\xi^k} \{H_{\rm eff} - \xi\}^k, \qquad (1)$$

where $H_{\rm BH}$ and $\hat{Q}$ are the Bloch-Horowitz Hamiltonian and the so-called $\hat{Q}$-box [36, 37], respectively. The latter contains only linked and unfolded Feynman-Goldstone diagrams in MBPT. The quantity ξ is a parameter (the origin of the $\hat{Q}$-box expansion), and the poles of $\hat{Q}(\xi)$ can be avoided with its appropriate value.

We renormalize the NN interaction using the so-called $V_{{\rm low}k}$ approach with a cutoff 2.0 fm^{-1} [40, 41, 42]. We solve Eq. (1) with a harmonic oscillator basis with the oscillator parameter $\hbar\omega = 45A^{-1/3} - 25A^{-2/3}$MeV=12.10 MeV where $A = 28$ ($A = Z{+}N$). The $\hat{Q}$-box is calculated up to the third order in eq. (1) and intermediate excitations up to 17 $\hbar\omega$ are included to guarantee convergence in the sum over intermediate states. Three-nucleon forces are included through the Fujita-Miyazawa term with its strength given by a standard π-N-Δ coupling [43]. This term is in turn transformed into a medium-dependent two-body interaction, see Refs. [28, 39, 44] for details.

The single-particle energies (SPEs) in the *sdpf* space are input too. Present chiral interactions result in too large shell gaps for the SPEs. In this work we employ ^{16}O as the closed-shell core and fit the values of SPEs to selected observables such as ground-state energies of $N <$ 20, ^{34}Si 2_1^+ level, *etc.* The energies of the 2p$_{1/2}$ and the 1f$_{5/2}$ orbits are constrained by the GXPF1 Hamiltonian of Ref. [10], due to lack of appropriate data. These SPEs, *i.e.*, one-body part of the Hamiltonian, will be confirmed to be reasonable, because effective SPEs to be calculated for Z=N=20 will turn out close to SPEs known for ^{40}Ca. The SPEs are isospin invariant, because of the ^{16}O core.

In this work we study Ne (Z=10), Mg (Z=12) and Si (Z=14) isotopes with a certain focus on $N \sim 20$ nuclei. Eigenvalues and eigenstates are obtained via standard Lanczos diagonalization method, including up to 8-particle-8-hole (8p8h) excitations from the *sd*-shell to the *pf*-shell. For the cases where the Lanczos diagonalization is infeasible (*e.g.*, $N > 22$) because of too large dimension, we switch to a Monte Carlo Shell Model calculation [45, 46].

The TBMEs vary gradually as a function of A because $\hbar\omega$ changes. Although TBMEs can be calculated for each nucleus explicitly, we introduce an overall scaling factor $(A/A_0)^{-0.2}$ with $A_0 = 28$. The value of the power is determined so that TBMEs calculated explicitly for several nuclei can be best reproduced by this simple parametrization.

Results and discussions. – Figure 1 shows the ground-state energies of Ne, Mg and Si isotopes. Since the Coulomb force is not included in the present effective interaction, its contribution estimated in a usual way is subtracted from experimental data. The results without 3NF are also plotted in Fig. 1.

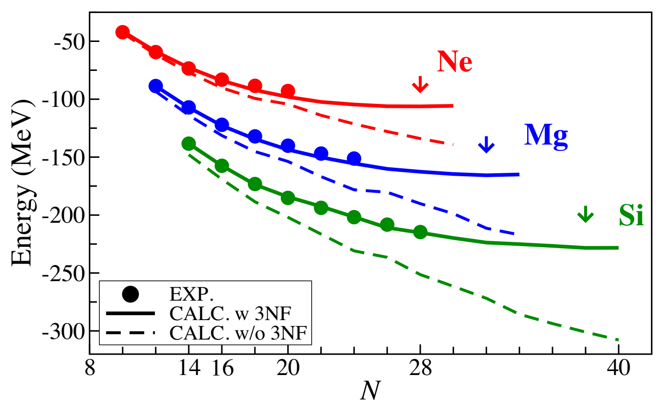

FIG. 1. (Color online) Ground-state energies of Ne, Mg and Si isotopes. Circles represent the experimental values. Shell-model results with (without) 3NF are shown by solid (dashed) lines. Arrows indicate the predicted drip lines. Experimental data are taken from Ref. [47]

Figure 1 indicates that the ground-state energies are reproduced quite nicely provided that 3NF effects are included. It is also worth noticing that the repulsion due to the 3NF grows as N increases in all the isotopic chains. This is consistent with earlier studies [28, 39]. We point out that this repulsion becomes stronger also as Z increases, suggesting that the present 3NF contribution is repulsive also in the proton-neutron channel. Figure 1 depicts the drip lines presently predicted [48, 49].

Figure 2 (a) shows the 2^+ and 4^+ energy levels. Experimental levels are well reproduced by the present calculation, including both gradual and steep changes as a function of N. For instance, the 2_1^+ level drops down as

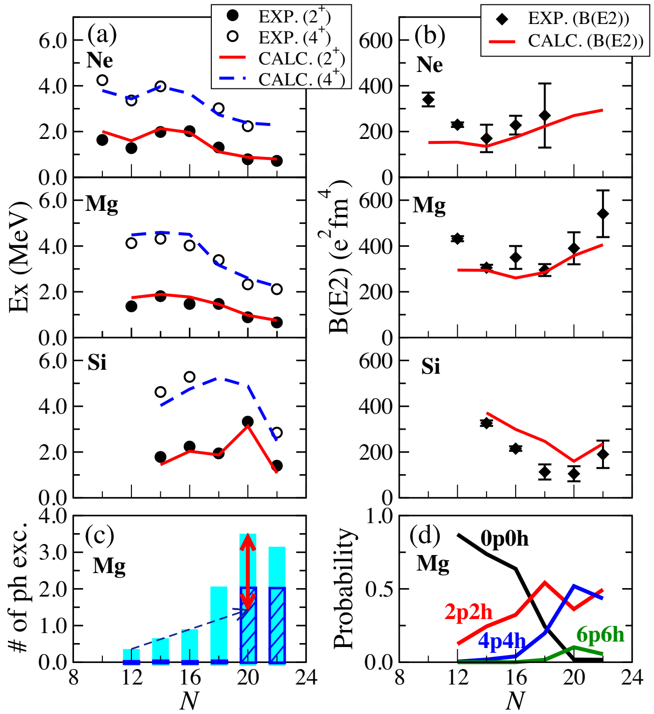

FIG. 2. (Color online) (a) Excitation energies of first 2^+ and 4^+ states and (b) $\mathrm{B}(\mathrm{E2}: 0_1^+ \to 2_1^+)$ values of Ne, Mg and Si isotopes. Experimental data (symbols) [47, 50] and present calculations (lines) are compared. (c) Expectation values of the number of the particle-hole excitations in the ground state of Mg isotopes. The plain histograms are present results, while the hatched ones imply the value by [14]. The dashed line shows the trend. The two-way arrow indicates the additional 2p2h excitation (see the text). (d) Decomposition of ph-excitation probabilities for the ground state of Mg isotopes.

steeply as by ∼1 MeV from $N = 16$ to 18 in Ne chain, while a similar change occurs from $N = 18$ to 20 in Mg chain. The 4_1^+ level varies differently as functions of N. For instance, in Mg isotopes, from $N = 16$ to 18, it starts to come down whereas the 2_1^+ level stays constant, implying that not only the degree of deformation but also the shape is changing. On the other hand, in Si isotopes, the 2_1^+ level jumps up at $N = 20$. All these behaviors of excited levels are reproduced rather well by the present calculation. The low excitation energy of the 2_1^+ levels in ^{30}Ne and ^{32}Mg indicates that these nuclei are strongly deformed and that *sd*-to-*pf* particle-hole (ph) excitations over the $N = 20$ gap occur significantly. In contrast, the higher-lying 2_1^+ level of ^{34}Si suggests that those ph excitations are weakened there.

Figure 2 (b) shows $\mathrm{B}(\mathrm{E2}: 0_1^+ \to 2_1^+)$ values. With effective charges, $(e_p, e_n) = (1.25, 0.25)e$, calculated B(E2) values exhibit systematic behaviors in agreement with experiment. This agreement is, however, not as good as that obtained for the energy levels. This probably indicates the need to derive E2 operator using the same microscopic theory, which will be presented elsewhere. While the $N = 20$ shell closure in Si isotopes is evident also in B(E2) systematics, the B(E2) values of Ne and Mg isotopes are larger at $N = 20$ than at $N = 18$, a feature which is consistent with growing deformation mentioned with respect to the 2_1^+ level.

We now turn to properties of the wave functions of Mg isotopes. Figure 2 (c) depicts the expectation value of the number of particle-hole (ph) excitations over the Z=N=20 shell gap for the ground state. One notices the abrupt increase at N=18 and furthermore at N=20. These increases are associated with the onset of large deformation: more particles (predominantly neutrons) in the *pf*-shell and many holes in the *sd*-shell enhance collective motion towards more deformed nuclear shape. The average value of the ph excitations is about 3.5 for ^{32}Mg. This is a large number, compared to the conventional picture for ^{32}Mg being basically a 2p2h state [9, 14, 15, 16, 17]. The value assumed in Warburton-Brown-Becker's island-of-inversion model [14] is shown in Fig. 2 (c) as a reference. The basic trend remains unchanged in other shell-model calculations, although the actual values can be somewhat larger [9, 15, 16, 17].

In the present calculation, this ph value starts low (<0.5) at N=12, and increases almost monotonically to N=16. This increase is a "modest" effect of the effective interaction shifting nucleons between the two shells, *e.g.* pairing effects. Considering that the 2_1^+ level remains high (∼ 2 MeV) up to N=18, this ph excitation mode does not produce a strong deformation. We extrapolate it linearly up to N=20 in Fig. 2 (c). The difference between the extrapolated and actual values is about 2, which can be interpreted as an additional 2p2h excitation essential for promoting the strong deformation. Although this interpretation is intuitive, the 2p2h excitation on top of the "modest" correlation appears to be analogous to the 2p2h picture of the conventional approaches.

Figure 2 (d) shows more details of the ph excitations involved in the Mg ground states. The probability of the 0p0h configuration comes down slowly for $N \leq 16$, and drops down sharply after that. The 2p2h probability increases gradually until N=16. The 4p4h is negligible up to N=16, but increases abruptly for $N \geq 18$, especially for N=20. Note that the 2p2h probability even decreases at N=20. Such changes drive the nucleus towards stronger deformation by including higher ph configurations. The present work thus resolves, for the first time, the long-standing puzzle as to how *sd*-to-*pf* excitations occur, showing notable differences from conventional approaches.

In constructing effective NN interactions for the *sd*-shell, *e.g.* USD [8], certain effects of *sd*-*pf* ph excitations are renormalized into TBMEs within the *sd* shell. If an *sd*-*pf* interaction is constructed on top of this *sd*-shell interaction (almost) unchanged, such a renormalized fraction of those excitations should not appear explicitly. In

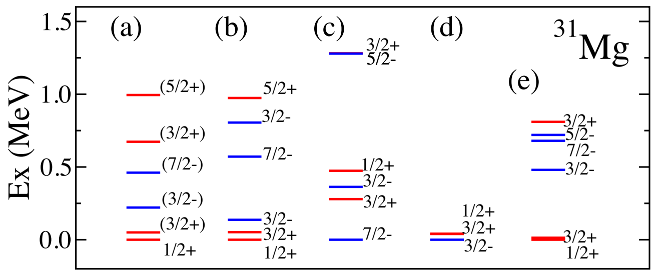

FIG. 3. Energy levels of ^{31}Mg. (a) experimental values, (b) present work, (c) sdpf-m [16], (d) sdpf-U-mix [17] and (e) AMD+GCM calculation [51], respectively.

fact, this is the case with the *sdpf-m* interaction (probably as well as others), with the above-mentioned expectation value being as small as 0.05, 0.08, 0.20, 0.85, 2.25 and 1.96 for $^{24-34}$Mg, respectively. In some cases, however, the explicit treatment of those excitations becomes crucial.

For transitional nuclei around ^{32}Mg, mixings of different ph configurations are indeed crucial, because the deformation contributes less to its binding energy. We show low-lying positive- and negative-parity levels of ^{31}Mg in Fig. 3. The present calculation reproduces the experimental levels rather well, for example, the ordering of lowest four levels. The configurations of the positive-party states are of 0p0h (normal) by 1-3%, 2p2h by 66-68%, and 4p4h by 29-30%. In contrast, the lowest $3/2^-$ and $7/2^-$ states are comprised of 33-35% 1p1h (normal), 55-57% 3p3h, and 11% 5p5h configurations. Thus, the ph properties differ significantly between positive- and negative-parity states, whereas similar ph excitations can be found within the same parity. It is clear that the coupling between different ph configurations has to be evaluated precisely. Figure 3 includes the results of other calculations. Among them, only the shell-model calculation of [17] reproduces the near-degeneracy of the three lowest levels, but it was mentioned that further fit of TBMEs was not attempted [17]. This is natural because of too many parameters with two major shells, while the present work generates all TBMEs from the underlying ground thanks to EKK method, being free from this kind of difficulty.

We briefly discuss a test of the present wave functions by transfer reactions. The spectroscopic factors are calculated as 0.77 and 1.41 for one-neutron removal from ^{32}Mg ground state to $3/2^-_1$ and $7/2^-_1$ states, respectively. The experimental values are 0.59(11) and 1.19(36) [52], respectively, which are in good agreement after scaling the theoretical values by the usual quenching factor ~ 0.7 [53, 54]. Thus, the present wave functions, which look different from those of conventional calculations, turn out to be quite consistent with these experimental values.

The last primary subject is the effective single-particle energy (ESPE). The ESPE represents the combined effect on the single-particle energies from the inert core and the monopole effects from other valence nucleons, producing important effects on the shell structure of exotic nuclei [5, 11, 12, 28]. Figure 4 shows the neutron ESPEs of the $N = 20$ isotones, calculated in the normal filling scheme, with and without 3NF and tensor force component. Here the tensor force component is extracted from a spin-tensor decomposition of the present NN effective interaction generated by the EKK method [27]. Figure 4 (a) indicates that the primary effect of 3NF is to raise all orbits by similar amounts [28]. Without 3NF effect, the neutron orbits are bound too deeply, yielding excessive binding energies, as seen in Fig. 1. On the other hand, Fig. 4 (b) demonstrates that the tensor force lowers or raises the ESPEs depending on the cases, and thereby change rather rapidly the spacing between certain orbits [11]. The ESPEs obtained at $N = 20$, including other $sd-pf$ orbits, appear to be reasonable for ^{40}Ca, suggesting the validity of input SPEs being used.

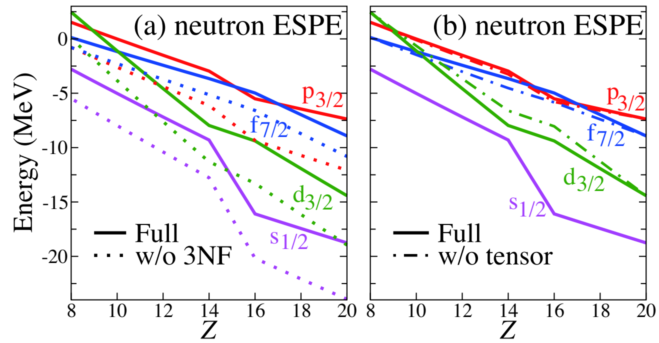

FIG. 4. (Color online) ESPEs of N=20 isotones for neutrons obtained in the normal filling scheme. Solid (dotted) lines in (a) show the case with (without) three-nucleon forces, while the solid (dot-dashed) lines in (b) represent the case with (without) the tensor force.

Figure 4 (a,b) indicates that the neutron *sd-pf* gap grows rapidly as Z increases from $Z = 8$ to $Z = 14$, and stays relatively constant after $Z = 14$ up to $Z = 20$ as being the $N = 20$ magic gap. This gap, however, disappears around $Z = 8$, and the $N = 16$ magic gap arises instead [55, 56, 57]. This is consistent with the trend shown by the simplified interaction, called VMU [12], where the central force gives a steady enlargement of the gap from $Z = 8$ to $Z = 20$, while the tensor force makes the change more rapid for $Z < 14$ but cancels the change for $Z > 14$. The neutron ESPEs of $f_{7/2}$ and $p_{3/2}$ at $Z = 20$ are also consistent of those of empirical interaction [16]. Two other upper orbitals, $p_{1/2}$ and $f_{5/2}$ appear at the energies similar to those of another empirical interaction [10], although not shown in Fig. 4. We thus demonstrate, for the first time, what type of shell evolution a chiral NN interaction such as the χN^{3}LO interaction produces in medium-mass exotic nuclei. It is seen also that the lowering as a function of Z is dampened by three-nucleon forces. The resulting trend is similar to that obtained with the VMU interaction of Ref. [12] as well as other interactions fitted to experiment [9, 16, 17].

Summary. –We have presented a microscopic description of neutron-rich nuclei Z=10-14 and N∼20, as the first application of EKK method to derive the effective interaction for actual cases. The calculated energies, B(E2) values and spectroscopic factors are in good agreement with experiment. While TBMEs are not fitted, the quality of the agreement is similar to or better than SM approaches with fitted TBMEs. Definite differences from conventional approaches are seen, particularly in the pattern of particle-hole excitations between the sd and pf shells. In this context, the conventional 2p2h picture of the island of inversion serves as an intuitive interpretation. We point out that the above-mentioned differences can be less, if ph excitations over the relevant magic gap are included explicitly in the fit of TBMEs like the case for pf+1$g_{9/2}$ orbit, *e.g.*, [58, 59]. The shell evolution is derived from the chiral EFT force and Fujita-Miyazawa 3-body force, for the first time. All these features contribute to further studies of exotic nuclei where microscopic theories play more crucial roles. Further progress in nuclear forces and many-body treatments will improve the agreement to experiment and provide us with more predictive power.

We thank Dr. Y. Utsuno for useful discussions. The Lanczos shell-model calculation is performed with the code "KSHELL" [60]. This work was supported in part by Grants-in-Aid for Scientific Research (23244049,15K05090). It was supported in part by HPCI Strategic Program (hp140210,hp150224,hp160221), in part by MEXT and JICFuS as a priority issue (Elucidation of the fundamental laws and evolution of the universe) to be tackled by using Post 'K' Computer, and also by CNS-RIKEN joint project for large-scale nuclear structure calculations.

[1] M. Mayer, Phys. Rev. **75**, 1969 (1949).
[2] O. Haxel, J. H. D. Jensen, and H. E. Suess, Phys. Rev. **75**, 1766 (1949).
[3] O. Sorlin and M. G. Porquet, Prog. Part. Nucl. Phys. **61**, 602 (2008).
[4] A. Gade and T. Glasmacher, Prog. Part. Nucl. Phys. **60**, 161 (2008).
[5] T. Otsuka, Phys. Scr. **T152**, 014007 (2013).
[6] S. Cohen and D. Kurath, Nucl. Phys. **73**, 1 (1965).
[7] T. T. S. Kuo and G. E. Brown, Nucl. Phys. **85**, 40 (1966).
[8] B. A. Brown, W. A. Richter, R. E. Julies, and B. H. Wildenthal, Annals of Physics **182**, 191 (1988).
[9] E. Caurier, G. Martínez-Pinedo, F. Nowacki, A. Poves, and A. P. Zuker, Rev. Mod. Phys. **77**, 427 (2005).
[10] M. Honma, T. Otsuka, B. A. Brown, and T. Mizusaki, Phys. Rev. C **65**, 061301 (2002).
[11] T. Otsuka, T. Suzuki, R. Fujimoto, H. Grawe, and Y. Akaishi, Phys. Rev. Lett. **95**, 232502 (2005).
[12] T. Otsuka, T. Suzuki, M. Honma, Y. Utsuno, N. Tsunoda, K. Tsukiyama, and M. Hjorth-Jensen, Phys. Rev. Lett. **104**, 012501 (2010).
[13] X. Campi, H. Flocard, A. K. Kerman, and S. Koonin, Nucl. Phys. A **251**, 193 (1975).
[14] E. K. Warburton, J. A. Becker, and B. A. Brown, Phys. Rev. C **41**, 1147 (1990).
[15] N. Fukunishi, T. Otsuka, and T. Sebe, Phys. Lett. B **296**, 279 (1992).
[16] Y. Utsuno, T. Otsuka, T. Mizusaki, and M. Honma, Phys. Rev. C **60**, 054315 (1999).
[17] E. Caurier, F. Nowacki, and A. Poves, Phys. Rev. C **90**, 014302 (2014).
[18] A. F. Lisetskiy, B. R. Barrett, M. K. G. Kruse, P. Navrátil, I. Stetcu, and J. P. Vary, Phys. Rev. C **78**, 044302 (2008).
[19] S. K. Bogner, H. Hergert, J. D. Holt, A. Schwenk, S. Binder, A. Calci, J. Langhammer, and R. Roth, Phys. Rev. Lett. **113**, 142501 (2014).
[20] G. R. Jansen, J. Engel, G. Hagen, P. Navrátil, and A. Signoracci, Phys. Rev. Lett. **113**, 142502 (2014).
[21] L. Coraggio, A. Covello, A. Gargano, and N. Itaco, Phys. Rev. C **87**, 034309 (2013).
[22] L. Coraggio, A. Covello, A. Gargano, and N. Itaco, Phys. Rev. C **89**, 024319 (2014).
[23] J. Simonis, K. Hebeler, J. D. Holt, J. Menéndez, and A. Schwenk, Phys. Rev. C rapid com. (in press).
[24] G. R. Jansen, A. Signoracci, G. Hagen, and P. Navrátil, arXiv:1511.00757v1 [nucl-th] (2015).
[25] K. Takayanagi, Nucl. Phys. A **852**, 61 (2011).
[26] K. Takayanagi, Nucl. Phys. A **864**, 91 (2011).
[27] N. Tsunoda, K. Takayanagi, M. Hjorth-Jensen, and T. Otsuka, Phys. Rev. C **89**, 024313 (2014).
[28] T. Otsuka, T. Suzuki, J. D. Holt, A. Schwenk, and Y. Akaishi, Phys. Rev. Lett. **105**, 032501 (2010).
[29] J. D. Holt, T. Otsuka, A. Schwenk, and T. Suzuki, J. Phys. G **39**, 085111 (2012).
[30] G. Hagen, M. Hjorth-Jensen, G. R. Jansen, R. Machleidt, and T. Papenbrock, Phys. Rev. Lett. **108**, 242501 (2012).
[31] G. Hagen, M. Hjorth-Jensen, G. R. Jansen, R. Machleidt, and T. Papenbrock, Phys. Rev. Lett. **109**, 032502 (2012).
[32] A. Ekström, G. R. Jansen, K. A. Wendt, G. Hagen, T. Papenbrock, B. D. Carlsson, C. Forssén, M. Hjorth-Jensen, P. Navrátil, and W. Nazarewicz, Phys. Rev. C **91**, 051301 (2015).
[33] T. T. S. Kuo, S. Y. Lee, and K. F. Ratcliff, Nucl. Phys. A **176**, 65 (1971).
[34] E. M. Krenciglowa and T. T. S. Kuo, Nucl. Phys. A **235**, 171 (1974).
[35] E. M. Krenciglowa, T. T. S. Kuo, E. Osnes, and P. J. Ellis, Nucl. Phys. A **289**, 381 (1977).
[36] T. Kuo and E. Osnes, Lecture Notes in Physics **364**, 1 (1990).
[37] M. Hjorth-Jensen, T. T. S. Kuo, and E. Osnes, Phys. Rep. **261**, 125 (1995).
[38] J. D. Holt, J. Menéndez, and A. Schwenk, Phys. Rev. Lett. **110**, 022502 (2013).
[39] J. D. Holt, J. Menéndez, J. Simonis, and A. Schwenk, Phys. Rev. C **90**, 024312 (2014).
[40] D. R. Entem and R. Machleidt, Phys. Rev. C **68**, 041001 (2003).
[41] S. Bogner, T. T. S. Kuo, L. Coraggio, A. Covello, and N. Itaco, Phys. Rev. C **65**, 051301 (2002).

[42] A. Nogga, S. K. Bogner, and A. Schwenk, Phys. Rev. C **70**, 061002 (2004).
[43] A. M. Green, Rep. Prog. Phys. **39**, 1109 (1976).
[44] J. D. Holt, J. Menéndez, and A. Schwenk, Eur. Phys. J. A **49**, 39 (2013).
[45] T. Otsuka, M. Honma, T. Mizusaki, N. Shimizu, and Y. Utsuno, Prog. Part. Nucl. Phys. **47**, 319 (2001).
[46] N. Shimizu, T. Abe, Y. Tsunoda, Y. Utsuno, T. Yoshida, T. Mizusaki, M. Honma, and T. Otsuka, Progress of Theoretical and Experimental Physics **2012**, 1A205 (2012).
[47] *NuDat (Nuclear Structure and Decay Data)*, URL http://www.nndc.bnl.gov/nudat2/.
[48] H. Koura, T. Tachibana, M. Uno, and M. Yamada, Prog. Theor. Phys. **113**, 305 (2005).
[49] J. Erler, N. Birge, M. Kortelainen, W. Nazarewicz, E. Olsen, A. M. Perhac, and M. Stoitsov, Nature **486**, 509 (2012).
[50] S. Takeuchi, M. Matsushita, N. Aoi, P. Doornenbal, K. Li, T. Motobayashi, H. Scheit, D. Steppenbeck, H. Wang, H. Baba, et al., Phys. Rev. Lett. **109**, 182501 (2012).
[51] M. Kimura, Phys. Rev. C **75**, 041302 (2007).
[52] J. R. Terry, B. A. Brown, C. M. Campbell, J. M. Cook, A. D. Davies, D. C. Dinca, A. Gade, T. Glasmacher, P. G. Hansen, B. M. Sherrill, et al., Phys. Rev. C **77**, 014316 (2008).
[53] A. Gade, P. Adrich, D. Bazin, M. D. Bowen, B. A. Brown, C. M. Campbell, J. M. Cook, T. Glasmacher, P. G. Hansen, K. Hosier, et al., Phys. Rev. C **77**, 044306 (2008).
[54] J. A. Tostevin and A. Gade, Phys. Rev. C **90**, 057602 (2014).
[55] B. A. Brown, Revista Mexicana de Fisica **39**, Suplemento 2, 21 (1993).
[56] A. Ozawa, T. Kobayashi, T. Suzuki, K. Yoshida, and I. Tanihata, Phys. Rev. Lett. **84**, 5493 (2000).
[57] T. Otsuka, R. Fujimoto, Y. Utsuno, B. A. Brown, M. Honma, and T. Mizusaki, Phys. Rev. Lett. **87**, 082502 (2001).
[58] M. Honma, T. Otsuka, T. Mizusaki, and M. Hjorth-Jensen, Phys. Rev. C **80**, 064323 (2009).
[59] Y. Tsunoda, T. Otsuka, N. Shimizu, M. Honma, and Y. Utsuno, Phys. Rev. C **89**, 031301 (2014).
[60] N. Shimizu, arXiv:1310.5431v1 [nucl-th] (2013).